Bulgarian Journal of Physics vol. **48** (2021) 174–182

Qubits, Decoherence and Edge State Detection: Illustration Using the SSH Model

M. Zaimi[1], **C. Boudreault**[2], **N. Baspin**[3], **H. Eleuch**[4], **R. MacKenzie**[5], **M. Hilke**[3]

[1]Centre de Recherches Mathématiques, Université de Montréal, C.P. 6128, succursale Centre-ville, Montréal, QC H3C 3J7, Canada
[2]Département des sciences de la nature, Collège militaire royal de Saint-Jean, 15 Jacques-Cartier Nord, Saint-Jean-sur-Richelieu, QC Canada, J3B 8R8
[3]Department of Physics, McGill University, Montréal, QC, Canada, H3A 2T8
[4]Department of Applied Sciences and Mathematics, College of Arts and Sciences, Abu Dhabi University, Abu Dhabi, UAE
[5]Département de physique, Université de Montréal, Complexe des Sciences, C.P. 6128, succursale Centre-ville, Montréal, QC, Canada, H3C 3J7

Received *May 7, 2020*

Abstract. As is well known, qubits are the fundamental building blocks of quantum computers, and more generally, of quantum information. A major challenge in the development of quantum devices arises because the information content in any quantum state is rather fragile, as no system is completely isolated from its environment. Generally, such interactions degrade the quantum state, resulting in a loss of information.

Topological edge states are promising in this regard because they are in ways more robust against noise and decoherence. But creating and detecting edge states can be challenging. We describe a composite system consisting of a two-level system (the qubit) interacting with a finite Su-Schrieffer-Heeger chain (a hopping model with alternating hopping parameters) attached to an infinite chain. In this model, the dynamics of the qubit changes dramatically depending on whether or not an edge state exists. Thus, the qubit can be used to determine whether or not an edge state exists in this model.

KEY WORDS: open quantum systems, decoherence, topological materials, edge states

 1310–0157 © 2021 Heron Press Ltd.

1 Introduction

The two-level system (TLS) is the simplest nontrivial quantum system. Its simplicity notwithstanding, many important systems are TLSs. Some familiar examples are: a spin-1/2 particle (two spin states), a photon (two polarizations), a two-level atom (the two levels), a quantum dot (empty/full), two-meson systems (K, $\bar{K}$), two-flavour neutrino oscillations ($\nu_{1,2}$). Some of the above play the role of qubits, the building blocks of quantum information systems (quantum computers, teleportation, etc).

An isolated TLS, like any isolated quantum system, will evolve unitarily. This implies that pure states remain pure; assuming the two basis states are coupled, a system put in one state will oscillate back and forth between the two.

However, no system is perfectly isolated; in reality, a TLS interacts with its environment and becomes entangled with it. From the point of view of the TLS, entanglement with the environment is indistinguishable from a mixed state. We say that the pure state becomes impure, or it decoheres. In addition, in many TLSs (including the one we will study here) the interaction can permit a particle to escape from the system to the environment. In this case, from the point of view of the TLS probability is not conserved.

Decoherence and nonconservation of probability are almost always undesirable; in particular, decoherence results in a loss of information and also a loss of the potential advantage of quantum vs classical computing, quantum vs classical communication, etc. Thus, understanding (and, usually, minimizing) decoherence is critically important to the functioning of quantum devices. As an example, in [1] a tripartite system was studied: a TLS coupled to one end of a finite chain (or channel) whose other end was coupled to a semi-infinite chain; both chains were described by tight-binding Hamiltonians. The question addressed was: how can one reduce the decoherence of the TLS? It was found that adding noise to the channel did the trick, essentially due to Anderson localization: if excitations in the channel are localized, it becomes hard for a particle in the TLS to make its way to the far side of the channel and escape to infinity.

Here, we study a similar system with a very different goal in mind (Figure 1). The main difference is that the channel is a Su-Schrieffer-Heeger (SSH) [2] chain (free of disorder) described by a hopping parameter with alternating hopping strengths. Such chains have topological edge states (for a review, see [3]), and rather than trying to minimize the decoherence of the TLS, we imagine measuring its decoherence rate to determine whether the system to which it is attached has edge states. As we will see, the presence of edge states greatly increases the decoherence rate.

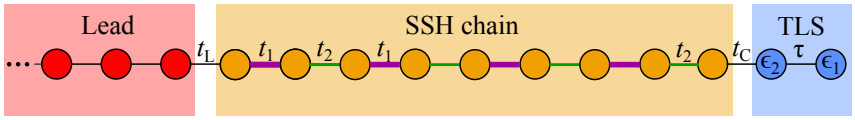

Figure 1. Tripartite system geometry. Rightmost SSH chain hopping parameter is t_1 or t_2 depending on whether number of sites N is even or odd, respectively (odd case shown here).

2 Two-Level System: A Brief Review

We review the isolated TLS, mostly to establish notation to be used in what follows. The TLS Hamiltonian is

$$H^{\mathrm{DD}} = \begin{pmatrix} \epsilon_2 & \tau \\ \tau & \epsilon_1 \end{pmatrix} \equiv \begin{pmatrix} \epsilon_0 - \delta_0/2 & \tau \\ \tau & \epsilon_0 + \delta/2 \end{pmatrix}. \tag{1}$$

The energies are $\lambda_\pm = \frac{1}{2}(\epsilon_1 + \epsilon_2 \pm \delta) = \epsilon_0 \pm \frac{\delta}{2}$, where $\delta = \sqrt{(\epsilon_1 - \epsilon_2)^2 + 4\tau^2}$. The energy-dependent Green's function is defined by $G^{\mathrm{DD}}(E) = (E - H^{\mathrm{DD}})^{-1}$; its Fourier transform gives the time-dependent Green's function, which is a sum of oscillatory terms with frequencies given by the energies; for instance,

$$G^{\mathrm{DD}}_{12}(t) = -\frac{2\pi i \tau}{\delta}\left(e^{-i\lambda_+ t} - e^{-i\lambda_- t}\right). \tag{2}$$

When we couple the TLS to the rest of the system, it will decohere; this will be seen in the Green's function, which will exhibit decaying behavior [1].

3 Su-Schrieffer-Heeger Model and Edge States

The SSH Hamiltonian [2], proposed in the context of the polymer polyacetylene for reasons we will not go into here, is

$$H_{\mathrm{SSH}} = \begin{pmatrix} 0 & t_1 & & & & \\ t_1 & 0 & t_2 & & & \\ & t_2 & 0 & t_1 & & \\ & & t_1 & 0 & \ddots & \\ & & & \ddots & \ddots & t \\ & & & & t & 0 \end{pmatrix}, \tag{3}$$

where $t = t_1$ or t_2 for N even or odd, respectively. We will assume $t_1, t_2 > 0$ for simplicity, and for now we assume N is even and write $N = 2M$. Much of what follows is known [4–7]; we repeat it to establish notation and to focus on results to be used below.

To solve the Schroedinger equation, translational invariance (by two sites) suggest the following ansatz:

$$|\psi\rangle = \sum_{n=0}^{M-1} \left(A\,|2n+1\rangle + B\,|2n+2\rangle\right) e^{in2k}. \tag{4}$$

We can take k between $\pm\pi/2$ since $k \to k+\pi$ has no effect on $|\psi\rangle$. The middle components of the Schroedinger equation (all but the first and last) determine the dispersion relation and also the ratio A/B. The former is

$$E^2 = t_1^2 + t_2^2 + 2\,t_1 t_2 \cos 2k. \tag{5}$$

Assuming k is real, $(t_1 - t_2)^2 < E^2 < (t_1 + t_2)^2$ so there are two energy bands. For any allowed energy, 5 has two equal and opposite solutions for $\pm k$ where we assume $k > 0$. Thus the general solution to the middle equations is a linear combination of the solutions for $\pm k$.

The edge components of the Schroedinger equation (the first and last) determine the ratio of these two solutions, and also the energy eigenvalues. The latter are given by the solutions of the following equation for k, where $r = t_1/t_2$ and we have written $\mathrm{s}_j = \sin(jk)$.

$$r\,\mathrm{s}_{N+2} + \mathrm{s}_N = 0. \tag{6}$$

where $r = t_1/t_2$ and we have written $\mathrm{s}_j = \sin(jk)$.

This equation cannot be solved analytically; however, numerically or graphically (see Figure 2) we find that there are N real solutions, as required, for $r > r_{\mathrm{C}}$ whereas there are two fewer real solutions for $r < r_{\mathrm{C}}$, where [4]

$$r_{\mathrm{C}} \equiv \frac{N}{N+2}. \tag{7}$$

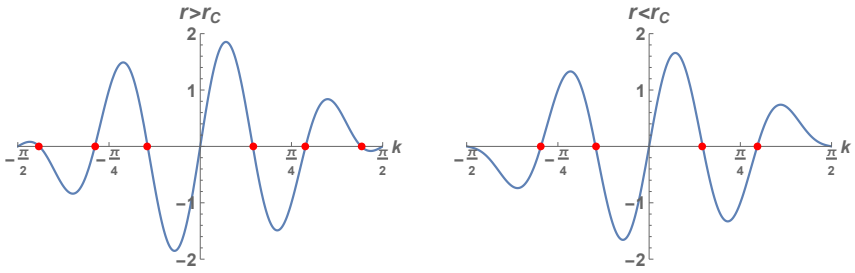

Figure 2. Graphical solution of (6) for $N = 6$ ($r_{\mathrm{C}} = 0.75$). Left panel: $r = 0.9$; six solutions. Right panel: $r = 0.7$; four solutions. (Note that $k = 0, \pm\pi/2$, although solutions of (6), do not correspond to solutions to the SE.)

Thus, for $r < r_C$ there are two missing solutions. These turn out to be solutions of complex wave number, $k = \pi/2 \pm i\kappa$, where κ is the positive solution of

$$\frac{\sinh(N\kappa)}{\sinh((N+2)\kappa)} = r. \tag{8}$$

the solution of which is displayed in Figure 3 for various values of N. These states, having complex k, are exponentially confined to the edges of the system: they are edge states. Also displayed is $l = 1/\kappa$, the penetration length of the edge states. As $r \to r_C$ from below, we see that the length scale goes to infinity; the "edginess" of the edge states becomes irrelevant if $l \gg N$.

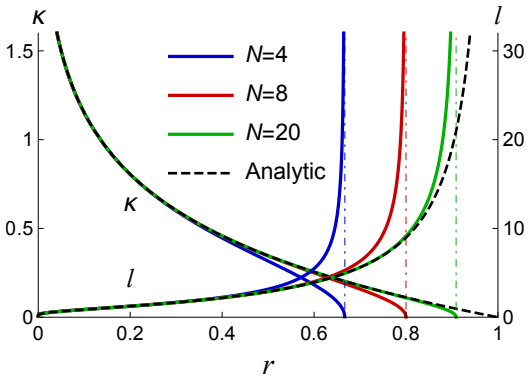

Figure 3. Decay rate κ and decay length l of edge states for various values of N. Also displayed is an analytic solution to (8) for $N \to \infty$.

We conclude with a brief discussion of the case N odd, which is in fact much simpler. It is easy to show that no matter the value of r, there is always exactly one zero-energy edge state (the remainder of the spectrum being symmetric). This state is confined to the left (right) edge for $r < 1$ ($r > 1$) with decay length $l = 2/|\log r|$. Figure 4 displays the spectra for $N = 20$ and 21.

4 Tripartite System: Chain-SSH-TLS

We now study the tripartite system displayed in Figure 1. Although it is an infinite-dimensional system, the effects of the SSH chain and semi-infinite chain on the TLS can be nicely incorporated into a 2×2 effective Hamiltonian for the TLS; these effects are simply given by a term added to the $(1,1)$ component of the Hamiltonian [7, 8]:

$$\epsilon_2 \to \epsilon_2 + \Sigma_{\mathrm{SSH},\infty} \equiv \epsilon_2'. \tag{9}$$

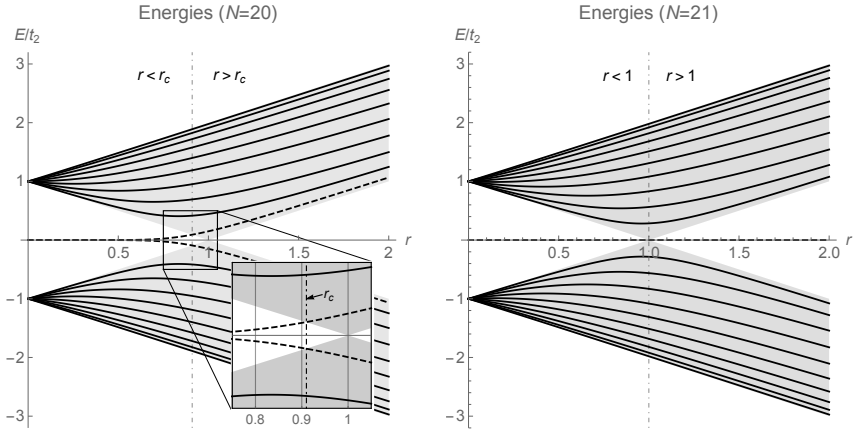

Figure 4. Energy spectra for two values of N as a function of r. The shaded regions are the bands for $N = \infty$. Dotted lines outside the bands are edge states. The inset on the left focuses on the transition between an edge state (to the left of the vertical broken line) and a non-edge state (to the right, in the shaded region).

Here $\Sigma_{\mathrm{SSH},\infty}$ is proportional to the surface Green's function of the combined SSH chain and semi-infinite chain. This can be calculated analytically, although it is fairly nasty. The result is [7]

$$\Sigma_{\mathrm{SSH},\infty} = \begin{cases} {t_\mathrm{C}}^2 \dfrac{Et_2 s_N - \Sigma_\infty(t_1 s_{N-2} + t_2 s_N)}{t_2^2(t_1 s_{N+2} + t_2 s_N) - Et_2\Sigma_\infty s_N} & (N \text{ even}) \\ {t_\mathrm{C}}^2 \dfrac{t_2(t_2 s_{N-1} + t_1 s_{N+1}) - E\Sigma_\infty s_{N-1}}{t_1 t_2 E s_{N+1} - t_1\Sigma_\infty(t_2 s_{N+1} + t_1 s_{N-1})} & (N \text{ odd}) \end{cases} \tag{10}$$

where

$$\Sigma_\infty = \frac{{t_\mathrm{L}}^2}{2}\left(E - i\sqrt{4 - E^2}\right). \tag{11}$$

Note that ϵ_2' is complex, so the effective Hamiltonian is no longer Hermitian. This is related to the open nature of the TLS: being non-Hermitian, time evolution preserves neither probability nor purity, reflecting the fact that the particle can escape to its environment, and that the TLS and environment become entangled.

Defining $\lambda_\pm'$ and δ' as the quantities defined in Section 2 with the substitution (9), we can use these substitutions in the definition of $G^{\mathrm{DD}}(E)$ given earlier to get the new energy-dependent Green's function, $G^{\mathrm{DD}}_{\mathrm{SSH},\infty}(E)$. It is tempting to suppose that these substitutions also work for the time-dependent Green's function. This is not quite correct, since $\lambda_\pm'$ depend in a highly nontrivial way on E so the Fourier transform cannot be evaluated exactly. An analytical approximation which is justified in the weak-coupling limit ($t_\mathrm{C} \ll 1$) [1] indicates that

to a good approximation the new (complex) frequencies $\lambda'_{\pm}$ can be evaluated at the old frequencies: the time-dependent Green's function has, according to this approximation, frequencies $\lambda'_{\pm}(\lambda_{\pm})$. According to this analytic approximation, the decay rates are given by the imaginary part of the frequencies, and we conclude that the decoherence time τ_ϕ is given by

$$(\tau_\phi)^{-1} \approx \min\left(-\frac{1}{2}\Im\left\{\Sigma_{\mathrm{SSH},\infty}(\lambda_{\pm}) \pm \delta'(\lambda_{\pm})\right\}\right). \tag{12}$$

This analytical approximation can be justified post hoc by comparing (12) with a numerical evaluation of the decoherence rate. Both are displayed in Figure 5. The figure, which encapsulates our main result, merits some discussion. There are four cases to consider, two for each graph.

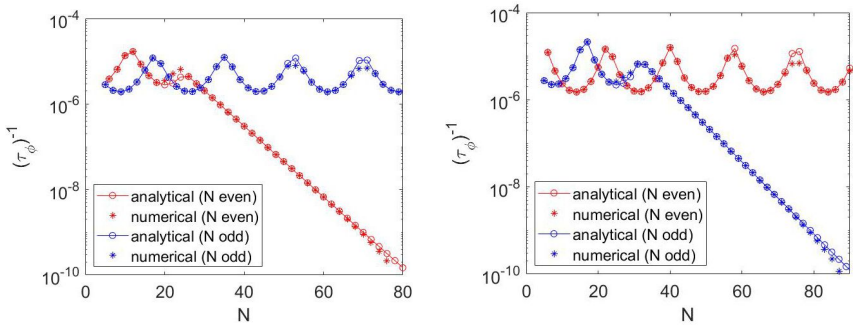

Figure 5. Decoherence rate as a function of N for $t_1 = 1/t_2 = 1.1$ (left), $t_2 = 1/t_1 = 1.1$ (right). For both figures, $(\epsilon_1, \epsilon_2, \tau, t_{\mathrm{C}}, t_{\mathrm{L}}) = (.4022, .0022, .03, .035, .65)$. The values for $\epsilon_{1,2}$ were chosen so that the isolated TLS has a zero eigenvalue, corresponding exactly (N odd) and approximately (N even) to the edge state energy. The energy of the other TLS state lies in the SSH gap.

The graph on the left corresponds to $r = 1.21$, for which there are no edge states if N is even, while there is a right edge state if N is odd. If N is even, both TLS states lie in the gap, so there are no SSH states with which they can hybridize. Thus, the SSH chain represents a sort of potential barrier impeding escape of the particle to the semi-infinite chain. As a result, the tunneling rate decreases exponentially with N beyond about 20. If N is odd (blue, upper curve), the right-hand edge state couples strongly to the TLS forming a pair of hybridized wave functions which penetrate the SSH chain. This penetration facilitates decoherence, and the rate remains large as N increases. Since the hybridized wave function itself drops off exponentially away from the right edge of the SSH chain, its effect on decoherence drops off as N increases; although this is not apparent in Figure 5, if we continue the graph beyond about $N = 120$, this effect is clearly seen [7]: eventually the blue curve on the left drops much like the red one does.

The graph on the right corresponds to $r \simeq 0.83$, for which there are two edge states if N is greater than 10 and even, while there is a left edge state if N is odd. Again, the behavior is dramatically different for even vs. odd parity. If N is even (red, upper curve), the presence of edge states results in hybridized wave functions which facilitate decoherence. As was discussed above ($r = 1.21$, N even), the decoherence is relatively independent of N until around $N = 120$, after which it drops exponentially. If N is odd (blue, lower curve), the absence of an edge state on the TLS side of the SSH chain impedes hybridization and giving rise to exponential decoherence suppression as N increases starting around $N = 30$.

While we believe the presence or absence of edge states explains in general terms the behavior exhibited in Figure 5, one unresolved issue is why the dropoff in decoherence begins where it does. It is easy to show that for the parameters used the edge states have a characteristic width of about ten sites, so it is puzzling why the enhanced decoherence illustrated by the upper curves persists until beyond $N = 100$.

5 Conclusions

The interaction between a TLS and its environment can have a strong effect on the dynamics of the TLS. Here, we argued that coupling to one end of an SSH chain (which is coupled at the other end to an undimerized infinite chain) can have a very strong effect on the decoherence of the TLS. The effect is dramatically different depending on whether there is or is not an edge state at the TLS end of the SSH chain: an edge state causes decoherence to remain high independent of chain length, wereas in the absence of an edge state decoherence decreases exponentially with chain length. This suggests using a TLS as a sort of edge state detector.

Acknowledgments

Talk given by R.M. at the Bahamas Advanced Studies Institute and Conferences (BASIC) 3rd Workshop on Solitons, Instantons, and other Topological Features, February 2020. This work was supported in part by the Natural Science and Engineering Research Council of Canada and by the Fonds de Recherche Nature et Technologies du Québec via the INTRIQ strategic cluster grant. RM is grateful for the hospitality of Perimeter Institute where part of this work was carried out. Research at Perimeter Institute is supported by the Government of Canada through the Department of Innovation, Science and Economic Development and by the Province of Ontario through the Ministry of Research, Innovation and Science.

References

[1] H. Eleuch, M. Hilke, R. MacKenzie (2017) Probing Anderson localization using the dynamics of a qubit. *Phys. Rev. A* **95** 062114.

[2] W.P. Su, J.R. Schrieffer, A.J. Heeger (1979) Solitons in Polyacetylene. *Phys. Rev. Lett.* **42** 1698.

[3] M.Z. Hasan, C.L. Kane (2010) Colloquium: Topological insulators. *Rev. Mod. Phys*. **82** 3045.

[4] P. Delplace, D. Ullmo, G. Montambaux (2011) *Phys. Rev. B* **84** 195452.

[5] J.K. Asbóth, L. Oroszlány, A. Pályi (2016) "*A short course on topological insulators*": Lecture Notes in Physics, Vol. 919 (Springer International Publishing).

[6] C. Duncan, P. Öhberg, M. Valiente (2018) *Phys. Rev. B* **97** 195439.

[7] M. Zaimi, C. Boudreault, N. Baspin, H. Eleuch, R. MacKenzie, M. Hilke (2019) arXiv:1910.09926 [cond-mat.mes-hall].

[8] S. Datta (2005) "*Quantum transport: atom to transistor*" (Cambridge University Press).